



## Research articles

# Effect of Cu/Fe/Co substitution on static and dynamic magnetic properties of Ni-Mn-Sn alloy thin films

Rajkumar Modak<sup>a</sup>, V.V. Srinivasu<sup>b</sup>, A. Srinivasan<sup>a,b,\*</sup><sup>a</sup> Department of Physics, Indian Institute of Technology Guwahati, Guwahati 781039, India<sup>b</sup> Department of Physics, University of South Africa, Johannesburg 1710, South Africa

## ARTICLE INFO

## Keywords:

Heusler alloy  
Thin film  
DC sputtering  
Gilbert damping  
Ferromagnetic resonance

## ABSTRACT

Cu or Fe or Co substituted off-stoichiometric Ni-Mn-Sn films of 500 nm thickness were deposited on Si (1 0 0) substrate by dc magnetron sputtering at ambient temperature and then annealed *ex situ* at 550 °C for 1 h under high vacuum. X-ray diffraction and atomic force microscopy analyses showed that the annealed films exhibited high degree of crystalline order with cubic  $L2_1$  phase. Magneto-static evaluation of the films established room temperature ferromagnetic order with easy axis of magnetization along the film plane in all the annealed films. The ratio of magnetic resonance and magnetic saturation ( $M_r/M_s$ ) increased drastically upon Co substitution. The analysis of polar angle dependence resonance field ( $H_r$ ) and resonance linewidth ( $\Delta H$ ) measurement using resonant cavity FMR technique revealed the presence of negative effective perpendicular magnetic anisotropy ( $K_1$ ) and very low Gilbert damping constant ( $\alpha$ ) in all the films.

## 1. Introduction

Off-stoichiometric Ni-Mn-Sn Heusler alloys have drawn the attention of researchers by their multifarious physical properties such as giant magnetoresistance, magnetic-field-induced phase transition, giant inverse magneto-caloric effect (MCE), giant magneto-thermal conductivity, giant Hall effect, large exchange bias, shape memory effect, and magnetic superelasticity effect [1–8]. A survey of the literature shows that most attention has been given to the study of the MCE in bulk Heusler alloys at the martensitic transition over the past decade and very little information is available on the thin film form of these alloys. It has been observed that these alloys have vast potential for application in room temperature environmental friendly refrigeration technology in bulk or thin film forms [9–12]. Apart from MCE, these alloy films exhibit other interesting properties which may find application in future technological devices. Recently, Ramudu et al. [13] observed large exchange bias (EB) in epitaxially grown Ni-Co-Mn-Sn film. Teichert et al. [13] demonstrated that Ni-Mn-Sn films can be used to induce unidirectional anisotropy in CoFeB/MgO/CoFeB magnetic tunnel junctions. Very low Gilbert damping constant with uniaxial anisotropy has been reported in Ni-Mn-Sn films [14,15]. Golub et al. [16] have provided a brief insight on antiferromagnetic coupling in the twinned martensite state of  $\text{Ni}_{46.0}\text{Mn}_{36.8}\text{Sn}_{11.4}\text{Co}_{5.8}/\text{MgO}(001)$  epitaxial thin film. These less explored attributes have opened up several novel applications for these films such as new generation magnetic

sensors, magnetic refrigeration, magnetic actuated devices and spintronic devices [13,15,17,18]. Proper estimation and control of parameters like magnetic anisotropy, magnetic exchange interactions, and intrinsic and extrinsic damping are necessary for using these alloy films as memory devices with high frequency response since these properties determine the efficiency and power consumption in spintronic and microelectronic devices [19]. Hence, understanding the magnetic relaxation processes in these thin films is one of the most interesting challenges in magnetism to date. Ferromagnetic resonance (FMR) is a powerful, non-destructive technique in microwave spectroscopy which allows the measurement of the amplitude, dynamics, and anisotropy of magnetization vector  $M$  and individual spins. FMR measurements are usually made using micro-strip line based FMR (MS-FMR) and resonance cavity based FMR (C-FMR). MS-FMR provides FMR data over a wide range of frequencies as well as a function of angular variation at a desired frequency. On the other hand C-FMR only allows angular variation at fixed frequency, which limits the accuracy of information obtained as compared to MS-FMR technique. But MS-FMR set-ups are mostly homemade and their sensitivity is strongly dependent on the quality of micro-strip line and good coupling with the detector. C-FMR methodology is based on commercial ESR setup with a high Q factor resonant cavity. Further, analysis of C-FMR data is simplified due to the microwave field uniformity over the sample and the absence of the microwave electric currents in the sample [20]. Both MS-FMR [21–23] and C-FMR [16,24–26] have used to study the magneto-dynamic

\* Corresponding author at: Department of Physics, Indian Institute of Technology Guwahati, Guwahati 781039, India.

E-mail addresses: [r.modak@iitg.ernet.in](mailto:r.modak@iitg.ernet.in) (R. Modak), [vallavs@unisa.ac.za](mailto:vallavs@unisa.ac.za) (V.V. Srinivasu), [asrini@iitg.ernet.in](mailto:asrini@iitg.ernet.in) (A. Srinivasan).

properties of magnetic materials as revealed by recent literature. This paper presents a systematic investigation of structural, (static and dynamic) magnetic properties of Ni-Mn-X-Sn ( $X = \text{Cu/Fe/Co}$ ) thin films deposited on Si (1 0 0) substrates.

## 2. Experimental details

Ni-Mn-Sn and Ni-Mn-X-Sn ( $X = \text{Cu, Fe, Co}$ ) Heusler alloy films were deposited on Si (1 0 0) substrate by dc magnetron sputtering from a 2 in. diameter and 1 mm thick  $\text{Ni}_{50}\text{Mn}_{37}\text{Sn}_{13}$  alloy target. Optimized values of working (Ar) gas pressure of 0.6 Pa and dc power of 10 W were maintained throughout the deposition process. The fourth element (X) was introduced in the films by symmetrically placed  $2 \times 2 \text{ mm}^2$  X chips on the Ni-Mn-Sn target. Before deposition, the sputtering chamber was evacuated to a base pressure better than  $10^{-4}$  Pa. As-deposited films were annealed *ex situ* at  $550^\circ\text{C}$  under residual Ar gas pressure of  $10^{-3}$  Pa for 1 h. Thickness of the films were measured with a surface profiler (Veeco Dektak 150) and was found to be  $500 \pm 5$  nm. Room temperature crystal structure of the films was determined using a rotating anode based X-ray diffractometer (Rigaku TTRAX III) with Cu  $K_\alpha$  radiation ( $\lambda = 0.15406$  nm) operated in grazing-incidence parallel beam mode. Composition of the films was evaluated using an energy dispersive X-ray spectroscopy unit (EDX, Oxford) attached to a field emission scanning electron microscope (FESEM, Zeiss Sigma). Surface morphology of the films was imaged at room temperature using an atomic force microscope (AFM, Bruker, Innova series). Magneto-static properties of the films were measured using a vibrating sample magnetometer (VSM, Lakeshore 7410) equipped with a closed cycle refrigerator for low temperature measurements. Magnetic field variation of the microwave absorption was recorded at room temperature for film orientations ranging from  $0$  to  $90^\circ$  with respect to magnetic field direction using an electron spin resonance (ESR) spectrometer (Bruker EMX EPR) operating at  $9.44$  GHz with a frequency modulation of  $100$  kHz. Thin film samples cut to  $\sim 2 \text{ mm} \times 2 \text{ mm}$  size were firmly placed on the flat tail of a fused silica sample rod. The sample rod, which could be manually positioned with  $\pm 1^\circ$  angular precision using a rotary mechanism, was inserted into the microwave cavity of the ESR spectrometer to record microwave absorption spectra as a function of film orientation to applied magnetic field.

## 3. Results and discussion

Room temperature x-ray diffraction (XRD) patterns of as-deposited films (not shown here) were amorphous in nature. After vacuum annealing at  $550^\circ\text{C}$  for 1 h, the amorphous films crystallized and the corresponding XRD patterns consisted of five Bragg peaks emanating from reflections from the cubic lattice planes. Presence of (1 1 1) and (2 2 0) super-lattice peaks in the XRD patterns further confirmed the formation of single phase austenite structure with  $L2_1$  ordering (space group  $\text{Fm}\bar{3}\text{m}$ ) in the films (cf. Fig. 1). The XRD data were refined using Rietveld method. In the stoichiometric  $\text{Ni}_2\text{MnSn}$  compound with  $L2_1$  structure and  $\text{Fm}\bar{3}\text{m}$  space group, the Ni, Mn and Sn atoms occupy the Wyckoff positions 8c ( $1/4, 1/4, 1/4$ ), 4b ( $1/2, 1/2, 1/2$ ) and 4a ( $0, 0, 0$ ), respectively, as shown in Fig. 2.(a). In off-stoichiometric  $\text{Ni}_{58.1}\text{Mn}_{34.4}\text{Sn}_{7.5}$ , the excess Mn and Ni atoms are presumed to occupy the Sn-sublattice as pointed out earlier [27,28]. The fourth element (X) atoms are assumed to occupy the Sn-sublattice by replacing the Ni and/or Mn atoms in those sites (see Fig. 2(b and c)). The refined patterns are shown in Fig. 1. In the figure, open circles represent the experimental diffraction data ( $Y_{\text{obs}}$ ) and the solid line corresponds to the fit obtained by Rietveld refinement method ( $Y_{\text{cal}}$ ) using the ‘FullProf’ open source software [29,30]. The goodness of the fit from which the crystallographic parameters of the films were extracted can be inferred from the difference data ( $Y_{\text{obs}} - Y_{\text{cal}}$ ) and  $\chi^2$  values provides in the figures. The average crystallite (grain) size (D) of the films has been calculated using Scherrer’s equation [31],

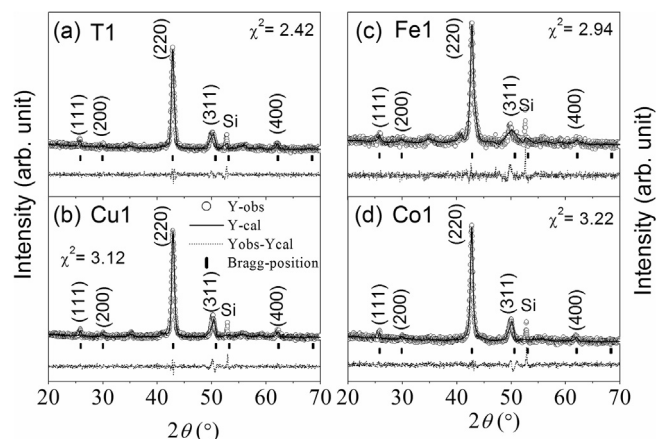


Fig. 1. Rietveld refined XRD patterns of annealed ternary and quaternary alloy films.

$$D = k\lambda/\beta\cos\theta \quad (1)$$

using the most intense (2 2 0) peak. Here,  $\beta$  is the full width at half maximum (FWHM) of the peak,  $k$  is a constant,  $\lambda$  is the incident wavelength and  $\theta$  is the diffraction angle. The FWHM determined from the refinement procedure has been used in Eq. (1) to evaluate D. Structural parameters evaluated from the XRD patterns are listed in Table 1. AFM images of the surface morphology of the films mapped over  $2 \times 2 \mu\text{m}^2$  scan area are shown in Fig. 3(a–d). The average surface roughness ( $R_a$ ) of the films was found to be 1.05, 1.42, 1.39 and 1.40 nm for T1, Cu1, Fe1 and Co1, respectively. It is evident that  $R_a$  increases upon substitution of the fourth element.

Room temperature magnetic properties of both as-deposited and annealed Ni-Mn-X-Sn thin films were studied using VSM at room temperature with an applied field cycle of  $\pm 10$  kOe. The room temperature isothermal magnetization versus applied field ( $M$ - $H$ ) curves (not shown here) of all the as-deposited films exhibited paramagnetic behavior which can be attributed to the amorphous or poor-crystalline nature of the films. However, upon annealing, ferromagnetic order is induced in the films with the formation of a polycrystalline structure. It is well known that the magnetism in these materials is closely related to the microstructure, atomic structure and the exchange interaction between the magnetic elements present in the alloy [32,33]. Though no significant change in saturation magnetization is observed upon Cu/Fe/Co substitution, the  $M$ - $H$  loop shape of the films changed noticeably. This may be due to change in the exchange interaction between the atoms in the unit cell induced by the substituent (X) element since the nature of the exchange coupling between the magnetic ions depends on their type and distance between them [32,33]. A careful look at the  $M$ - $H$  loops (cf. Fig. 4(a)) would reveal that the ternary (T1) and Cu substituted (Cu1) alloy films exhibit almost similar magnetic behavior, whereas the Fe substitute (Fe1) and Co substituted (Co1) alloy films show more softer loops with increasing  $M_r/M_s$  ratio. Hence, the presence of small amounts of non-magnetic (X) element in the unit cell of Ni-Mn-Sn alloy does not contribute much to the magnetic behavior of the alloy. However, the same amount of magnetic X (= Fe/Co) element in the unit cell is capable of considerably modifying the  $M$ - $H$  loop of the alloy film.

Fig. 4(b) represents  $M$ - $H$  loops recorded with magnetic field applied along the film plane and perpendicular to the film plane. It is evident from the figure that it is easy to magnetize the films along the film plane or in other words, they have easy magnetization plane along the film plane. For T1, Fe1 and Cu1 films, a finite loop area is found for out of plane  $M$ - $H$  loops. The Co1 film shows a flat hard magnetic loop for the out of plane direction which confirms that all the domains is aligned along the film plane. The in plane and out of plane  $M$ - $H$  loops also indicate the presence of magnetic anisotropy in the films. The values of magnetic anisotropy constants can be determined more accurately from

Download English Version:

<https://daneshyari.com/en/article/8152605>

Download Persian Version:

<https://daneshyari.com/article/8152605>

[Daneshyari.com](https://daneshyari.com)